Engineering Analysis with Boundary Elements 36 (2012) 858–865

Contents lists available at SciVerse ScienceDirect

Engineering Analysis with Boundary Elements

journal homepage: www.elsevier.com/locate/enganabound

Isogeometric analysis in BIE for 3-D potential problem

Jinliang Gu [a], Jianming Zhang [a,b,*], Guangyao Li [a]

[a] State Key Laboratory of Advanced Design and Manufacturing for Vehicle Body, College of Mechanical and Vehicle Engineering, Hunan University, Changsha 410082, PR China
[b] State Key Laboratory of Structural Analysis for Industrial Equipment, Dalian University of Technology, Dalian 116023, PR China

ARTICLE INFO

Article history:
Received 9 August 2011
Accepted 24 September 2011
Available online 7 December 2011

Keywords:
Isogeometric analysis
B-spline basis functions
NURBS
BIE

ABSTRACT

The isogeometric analysis is introduced in the Boundary Integral Equation (BIE) for solution of 3-D potential problems. In the solution, B-spline basis functions are employed not only to construct the exact geometric model but also to approximate the boundary variables. And a new kind of B-spline function, i.e., local bivariate B-spline function, is deducted, which is further applied to reduce the computation cost for analysis of some special geometric models, such as a sphere, where large number of nearly singular and singular integrals will appear. Numerical tests show that the new method has good performance in both exactness and convergence.

Contents

1. Introduction . . . 858
2. B-spline, NURBS and local B-spline . . . 859
   2.1. Basis functions . . . 859
   2.2. Local basis functions . . . 859
   2.3. Bivariate B-spline and NURBS function . . . 860
   2.4. Local bivariate B-spline function . . . 860
3. Implementation of isogeometric analysis in BIEs . . . 860
   3.1. BIEs for 3-D potential problem . . . 860
   3.2. B-spline approximation . . . 861
   3.3. Exact geometric information . . . 861
4. Numerical examples . . . 862
   4.1. Potential problem for a sphere shell . . . 862
   4.2. Potential problem for a tube . . . 863
5. Conclusions . . . 864
   Acknowledgments . . . 864
   References . . . 864

1. Introduction

The conception of isogeometric analysis was first introduced by Hughes et al. [1] and further developed by Cottrell et al. [2,3], Bazilevs et al. [4,5], and Zhang et al. [6]. Its goals are to generalize and improve on Finite Element Analysis (FEA) in following aspects: (1) To provide exact geometry for analysis no matter how coarse the discretization. (2) To simplify mesh refinement by eliminating the need for communication with the CAD geometry once the initial mesh is constructed. (3) To more tightly weave the mesh generation process within CAD. Within the concept, basis functions generated from non-uniform rational B-spline (NURBS) play a key role in offering exact geometry representation, simplification of design optimization and tighter integration of analysis and CAD. Although NURBS is not the unique tool for implementation of isogeometric analysis, it is the one in the most widespread use so far. It may be owing to the two facts, one is that NURBS is the standard approach for representation of free form curves and sculptured surfaces in CAD, and can represent elementary shapes such as sphere, cylinders, and torus exactly. These make it possible for NURBS to express all of CAD models in

* Corresponding author at: State Key Laboratory of Advanced Design and Manufacturing for Vehicle Body, College of Mechanical and Vehicle Engineering, Hunan University, Changsha 410082, PR China. Tel.: +86 731 8823061.
E-mail address: zhangjm@hnu.edu.cn (J. Zhang).

0955-7997/$ - see front matter © 2011 Elsevier Ltd. All rights reserved.
doi:10.1016/j.enganabound.2011.09.018

a uniform geometric representation. Another is that the basis functions originated in the field of approximation theory and inherently have some useful mathematic and geometric properties, such as the local support, nonnegative and partition of unit. These are attractive properties with regard to numerical stability. Following the development of NURBS based isogeometric analysis, one challenging but trivial task still needed for resolution is how to efficiently and exactly generate a trivariate NURBS solid from a given bivariate NURBS surface [7].

Considering the meaningful influence of isogeometric analysis, we first introduce the conception into the Boundary Element Analysis (BEA) [8–11] to solve 3-D potential problem. In our scheme, basis functions of B-spline or NURBS are used to construct CAD model and approximate boundary variables in BIE in the same parametric space. Because of the explicit B-spline expression, the geometric information for solution of BIE can be directly calculated from the CAD model. So no matter how coarse the mesh is, the boundary information is exact. This is a distinct advantage over the traditional Boundary Element Method (BEM) where the geometric model for BEA is from element approximation. The BEA is a dimensional reduction method. For 3-D potential problem, the 3-D geometric bodies for analysis are based on the Boundary representation (B-rep) [12,13]. And only boundary surfaces information is needed for the solution of BIE. So isogeometric analysis in BEA is much more easy to be implemented compared with that for FEA. The challenging problem mentioned above that is difficulty in the 3-D modeling can also be avoided here.

Nearly singular and singular integrals are key factors to deteriorate the exactness of numerical results in BEA. Because of tensor product restriction, the mesh in BEA for discretization of 3-D B-spline boundary surfaces must be kept in an uniform rectangular-grid in isogeometric analysis. For some bodies, this fashion of mesh can result in many singular points appearing in the body boundary surface, such as the tensor product fashion of mesh in a sphere. The appearance of these points lead to many nearly singular and singular integral required for evaluation. To overcome this drawback, we develop a local bivariate B-spline function based on the B-spline basis definition. This kind of B-spline largely alleviates the influence of global tensor product, and allows free allocation of the element number in one of the parametric directions.

It is worthy of mentioning that before our work, the attempt for using exact geometric information in BEA has been performed. The method for implementation of it is called as Boundary Face Method (BFM) that first proposed by Zhang et al. [14]. In their scheme, the exact 3-D geometric models for analysis are based on B-rep, which is constructed by the CAD software, such as UG-NX. The approximation of boundary variables in BFM are performed in the same parametric space of CAD model that is similar with the isogeometric analysis. But the parametric expressions in CAD and in CAE are so different that the refinement needs iterative communication with CAD geometry.

This paper is organized as follows. In Section 2, there are expressions of B-spline and NURBS, and local B-spline functions. In Section 3, the implementation of isogeometric analysis in 3-D potential BIE is performed. Numerical examples for 3-D potential problems are given in Section 4. Finally, we present the conclusions for our work.

2. B-spline, NURBS and local B-spline

2.1. Basis functions

B-spline, NURBS and local B-spline are built from B-spline basis functions. These basis functions are defined recursively for zero degree

$$B_{i,k}(\xi)=\begin{cases}1, & \xi_i\le\xi\le\xi_{i+1}\\ 0, & \text{otherwise}\end{cases}\quad k=0 \tag{1}$$

and for non-zero degrees

$$B_{i,k}(\xi)=\frac{\xi-\xi_i}{\xi_{i+k}-\xi_i}B_{i,k-1}(\xi)+\frac{\xi_{i+k+1}-\xi}{\xi_{i+k+1}-\xi_{i+1}}B_{i+1,k-1}(\xi),\quad k>0 \tag{2}$$

Assuming that $0/0:=0$ and $\Xi=[\xi_1,\xi_2,\ldots,\xi_{n+k+1}]$, where Ξ is a knot vector; ξ_i the ith knot and n the total number of basis functions corresponding to the number of control points. Knot values presented in the knot vector Ξ are given by: $\xi_1=\xi_2=\cdots=\xi_{k+1}=0$, $\xi_{n+1}=\xi_{n+2}=\cdots=\xi_{n+k+1}=>1$, and $\xi_i=(i-(k+1))/(n-k)$ for $i=k+2,k+3,\ldots,n$.

2.2. Local basis functions

To use Eq. (2), it is easy to deduct the high degree basis functions. These basis functions are defined in the global knot interval in order, such as the cubic basis functions described in Fig. 1(a). Local B-spline basis function is the basis functions defined in one of non-zero knot subintervals, such as the superposed segments: $B^{(4)}_{3,3}(\xi)$, $B^{(3)}_{4,3}(\xi)$, $B^{(2)}_{5,3}(\xi)$ and $B^{(1)}_{6,3}(\xi)$ in the [0.4, 0.6] depicted in Fig. 1(b), $B^{(l)}_{i,k}(\xi)$ is the lth segment of the ith basis function.

The transformation of local B-spline basis functions from B-spline basis functions also can be depicted in a mathematic expression. For example, an intact two degree basis function defined in a local knot vector $[\xi_i,\xi_{i+1},\xi_{i+2},\xi_{i+3}]$ can be expressed as

$$B_{i,2}=\begin{cases}\frac{(\xi-\xi_i)^2}{(\xi_{i+2}-\xi_i)(\xi_{i+1}-\xi_i)}, & \xi_i\le\xi<\xi_{i+1}\\ \frac{(\xi-\xi_i)(\xi_{i+2}-\xi)}{(\xi_{i+2}-\xi_i)(\xi_{i+2}-\xi_{i+1})}+\frac{(\xi_{i+3}-\xi)(\xi-\xi_{i+1})}{(\xi_{i+3}-\xi_{i+1})(\xi_{i+2}-\xi_{i+1})}, & \xi_{i+1}\le\xi<\xi_{i+2}\\ \frac{(\xi_{i+3}-\xi)^2}{(\xi_{i+3}-\xi_{i+1})(\xi_{i+3}-\xi_{i+2})}, & \xi_{i+2}\le\xi<\xi_{i+3}\end{cases} \tag{3}$$

The values of this intact basis function in other non-zero subintervals of the global knot vector $\Xi=[\xi_1,\xi_2,\ldots,\xi_{n+k+1}]$ are zero, that is to say, the intact basis function is a global basis function, which only has definition in the local knot vector $[\xi_i,\xi_{i+1},\xi_{i+2},\xi_{i+3}]$. So we call this intact basis function as global B-spline basis function.

The basis function can be transferred into a local B-spline basis function defined in a non-zero knot subinterval $[\xi_i,\xi_{i+1})$, which

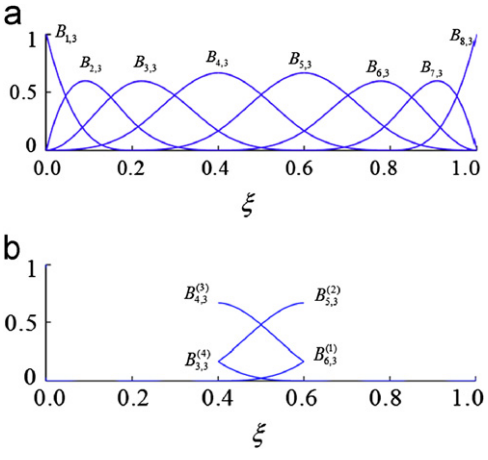

Fig. 1. Local B-spline basis functions located in the subinterval [0.4, 0.6].

can be expressed as

$$\begin{cases} B_{i-2,2}^{(3)}(\xi)=\frac{(\xi_{i+1}-\xi)^2}{(\xi_{i+1}-\xi_{i-1})(\xi_{i+1}-\xi_i)} \\ B_{i-1,2}^{(2)}(\xi)=\frac{(\xi-\xi_{i-1})(\xi_{i+1}-\xi)}{(\xi_{i+1}-\xi_{i-1})(\xi_{i+1}-\xi_i)}+\frac{(\xi_{i+2}-\xi)(\xi-\xi_i)}{(\xi_{i+2}-\xi_i)(\xi_{i+1}-\xi_i)} \\ B_{i,2}^{(1)}(\xi)=\frac{(\xi-\xi_i)^2}{(\xi_{i+2}-\xi_i)(\xi_{i+1}-\xi_i)} \end{cases} \tag{4}$$

The local B-spline basis function is a group of basis segments from several different global B-spline basis functions with the same location in a non-zero knot subinterval $[\xi_i,\xi_{i+1})$, $i\in\{k+1,\ldots,n\}$.

2.3. Bivariate B-spline and NURBS function

Given a control net $\{p_{ij}\}$ and two series of B-spline basis functions: $\{B_{i,k}(\xi)\}$ and $\{B_{j,l}(\eta)\}$, which are, respectively, located in the knot vectors $\Xi_1=[\xi_1,\xi_2,\ldots,\xi_{m+k+1}]$ and $\Xi_2=[\eta_1,\eta_2,\ldots,\eta_{n+l+1}]$, (here $i=1,2,\ldots,m$, $j=1,2,\ldots,n$), a bivariate B-spline function is defined by

$$P(\xi,\eta)=\sum_{i=1}^{m}\sum_{j=1}^{n}B_{i,k}(\xi)B_{j,l}(\eta)p_{ij} \tag{5}$$

and a bivariate NURBS function is defined by

$$P(\xi,\eta)=\sum_{i=1}^{m}\sum_{j=1}^{n}\frac{B_{i,k}(\xi)B_{j,l}(\eta)w_{ij}}{\sum_{i=1}^{m}\sum_{j=1}^{n}B_{i,k}(\xi)B_{j,l}(\eta)w_{ij}}p_{ij} \tag{6}$$

In Eq. (6), w_{ij} is the weight value corresponding to the tensor product $B_{i,k}B_{j,l}$. When all weights (i.e., w_{ij}) are set to 1, Eq. (6) degenerates into Eq. (5).

Because all of tensor product $B_{i,k}B_{j,l}$ are defined in the global knot vector: Ξ_1 or Ξ_2 (here we call this fashion of tensor product as global tensor product), each of parametric mesh mapped from control nets must be subdivided in uniform rectangular grid, such as that described in Fig. 2, which requires 4 row-grids in every column and 5 column-grids in every row. To distinguish the following definitions, we denote the expressions (3) and (4) as global bivariate B-spline and NURBS functions, respectively.

2.4. Local bivariate B-spline function

To use the global bivariate B-spline function to approximate the boundary variables in the BIEs, many extra nearly singular and singular integrals will appear on some particular body surfaces, such as the sphere surface in Fig. 3. This is a trickiness problem in the realm of BEM, which will deteriorate the final numerical results. The reason of their appearance is that the parametric domains of the surfaces are unsuitably meshed according to the global tensor product fashion of B-spline.

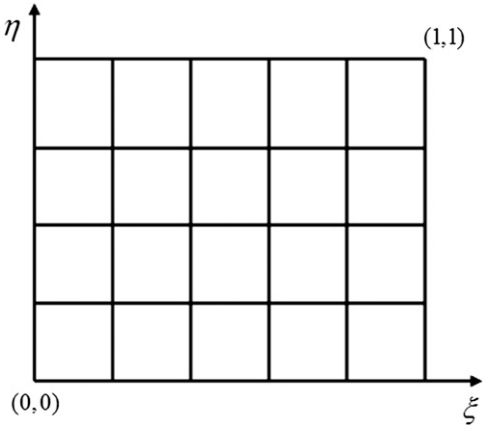

Fig. 2. A parametric mesh for a global bivariate B-spline or a NURBS function.

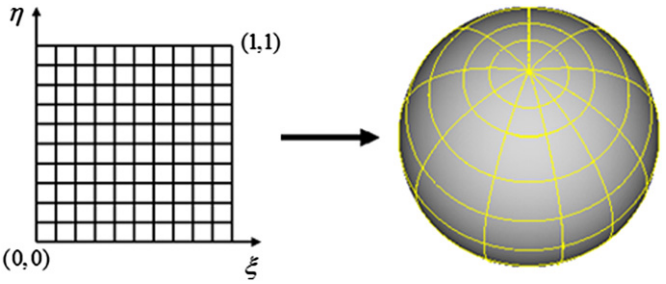

Fig. 3. Parameter mesh and surface mesh of a sphere according to the global tensor product fashion of B-spline.

It results in surplus elements huddling together in the areas of singular points, such as that in Fig. 3.

To use the local bivariate B-spline function, it is possible to avoid the computation of these integrals. The local bivariate B-spline function is an extension of PB-spline [15] into 2-D parametric space. It also can be considered as a special kind of T-spline [16], which allows free allocation of number of rectangular grids in one of the 2-D parametric directions. Its expression is written as

$$P(\xi,\eta)=\sum_{i=1}^{n}\sum_{j=1}^{m}B_{i,k}(\xi)B_{j,l}(\eta)p_{ij}=\sum_{r=0}^{k}\sum_{s=0}^{l}N_{rs}(\xi,\eta)p_{rs} \tag{7}$$

where $N_{rs}(\xi,\eta)$ is defined by

$$N_{rs}(\xi,\eta)=\begin{cases} B_{i_r-r,k}^{(r+1)}(\xi)B_{j_s-s,l}^{(s+1)}(\eta), & \xi\in[\xi_{i_r},\xi_{i_r+1}),\eta\in[\eta_{j_s},\eta_{j_s+1}) \\ 0, & \text{otherwise} \end{cases} \tag{8}$$

$p_{ij}(x_{ij},y_{ij},z_{ij})$ is from the control net $\{p_{ij}\}$. ξ and η are parametric coordinates with their values lying in the $[\xi_1,\xi_2,\ldots,\xi_{n+k+1}]$ and $[\eta_1,\eta_2,\ldots,\eta_{m+l+1}]$, respectively. $p_{rs}=p_{(i_r-r)(j_s-s)}$, $i_r\in\{k+1,\ldots,n\}$ and $j_s\in\{l+1,\ldots,m\}$. $[\xi_{ir},\xi_{i_r+1})$ and $[\eta_{j_s},\eta_{j_s+1})$ are non-zero knot intervals. $B_{i_r-r,k}^{(r+1)}(\xi)$ and $B_{j_s-s,l}^{(s+1)}(\eta)$ are the local B-spline basis function, which are defined in $[\xi_{i_r},\xi_{i_r+1})$ and $[\eta_{j_s},\eta_{j_s+1})$, respectively.

The local bivariate B-spline function is a particular kind of bivariate B-spline function. When its parameter mesh is subdivided with the fashion of the same row-grids in every column and the same column-grids in every row, it degenerates into global bivariate B-spline function.

3. Implementation of isogeometric analysis in BIEs

The isogeometric analysis is using the same mathematical tool to construct an exact geometric model in CAD and approximate physical variable in CAE in the same parametric space. Because this tool has an explicit expression, it is easy to obtain the exact geometric information for analysis. Here, B-spline basis function is used as the tool to implement the isogeometric analysis in the BIEs of 3-D potential problems.

3.1. BIEs for 3-D potential problem

Given the boundary conditions, the 3D potential problem governed by the Laplace's equation can be described as

$$\begin{cases} \nabla^2 u=0, & \forall x\in\Omega \\ u=\overline{u}, & \forall x\in\Gamma_u \\ q=\overline{q}, & \forall x\in\Gamma_q \end{cases} \tag{9}$$

where x is $x(x_1,x_2,x_3)$ in the Cartesian coordinates; the domain Ω with the closed boundary $\Gamma=\Gamma_u+\Gamma_q$; $\overline{u}$ and $\overline{q}$ are the prescribed

potential and normal flux, respectively, on the essential boundary Γ_u and natural boundary Γ_q; $q \equiv \partial u/\partial n$ is the flux on the boundary Γ along the outward normal direction of n.

Corresponding to the above partial differential equation, the self-regular BIE is written as

$$0 = \int_\Gamma (u(s)-u(y))q^s(s,y)d\Gamma - \int_\Gamma q(s)u^s(s,y)d\Gamma \tag{10}$$

where u and q are, respectively, the potential and flux function on the boundary Γ. S is the field point (integration point), y is the source point (collocation point). $u^s(s,y)$ and $q^s(s,y)$are the fundamental solutions. In 3-D potential problems

$$u^s(s,y) = \frac{1}{4\pi r(s,y)} \tag{11}$$

$$q^s(s,y) = \frac{\partial u^s(s,y)}{\partial n(s)} = \frac{1}{4\pi r^2(s,y)} \sum_{i=1}^{3} \frac{x_i(s)-x_i(y)}{r(s,y)} n_i(s) \tag{12}$$

where r is the distance from the source to the field point in Cartesian coordinates.

3.2. B-spline approximation

In the isogeometric analysis schema, both the bivariate B-spline surfaces to represent the integral boundary Γ of a body and the local bivariate B-spline function to approximate the boundary values: $u_j(s)$ and $t_j(s)$, are expressed in the parametric form. Therefore, the discretization of the Eq. (10) can be performed in the parametric domain. Fig. 4 shows a parametric mesh, which maps to a 3-D mesh model of a boundary surface. The red dots denote the parametric coordinates of nodes. The purple dashed mesh-grids are integral background elements, which are one-to-one corresponding to the nodes, for example the labeled domain of an integral element Γ_{uv}. The black mesh-girds are parametric subdivision according to the knot vectors of a quadratic bivariate B-spline: $\Xi_\xi = [0,0,0,1/3,2/3,1,1,1]$ and $\Xi_\eta = [0,0,0,1/2,1,1,1]$. The virtual values, considered as the control points of the B-spline function, are located on the corner points of each black grids, denoted by $\hat{p}_{ij}$. The node values are denoted by $\tilde{p}_{ij}$. Given boundary condition is imposed on these red dots.

To take use of the mesh fashion described as Fig. 3, Eq. (10) can be discreted as

$$0 = \sum_{uv} \int_{\Gamma_{uv}} (u(s)-u(y))q^s(s,y)d\Gamma(s) - \sum_{uv} \int_{\Gamma_{uv}} q(s)u^s(s,y)d\Gamma(s) \tag{13}$$

Note that u in $\sum_{uv}$ is only a subscript, which is different from the variable u or the basis function u^s.

Subsequently, the local bivariate B-spline function can also be constructed with $\hat{p}_{ij}$ as control points, which is expressed as

$$P(\xi,\eta) = \sum_{r=0}^{k} \sum_{s=0}^{l} N_{rs}(\xi,\eta)p_{rs} \tag{14}$$

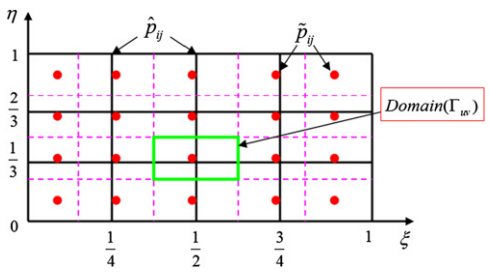

Fig. 4. Parametric mesh of an integral boundary B-spline surface. (For interpretation of the references to color in this figure, the reader is referred to the web version of this article.)

where $p_{rs} = \hat{p}_{(i_r-r)(j_s-s)}$, $i_r \in \{k+1,\ldots,n\}$ and $j_s \in \{l+1,\ldots,m\}$. In Fig. 4, $n=5$, $m=4$ and $k=l=2$. Eq. (14) can be expanded, which then is expressed as another form, such as

$$\begin{aligned} P(\xi,\eta) &= \sum_{r=0}^{k} \sum_{s=0}^{l} N_{rs}(\xi,\eta)p_{rs} \\ &= \sum_{r=0}^{k} N_{r0}(\xi,\eta)p_{r0} + \sum_{r=1}^{k} N_{r1}(\xi,\eta)p_{r1} + \cdots + \sum_{r=l}^{k} N_{rl}(\xi,\eta)p_{rl} \\ &= \sum_i N_i(\xi,\eta)\hat{p}_i \end{aligned} \tag{15}$$

where $N_i(\xi,\eta)$ and $\hat{p}_i$ are, respectively, the vector elements of $[N_i]$ and $[\hat{p}_i]$, which one- to-one correspond to the determinant elements of $[N_{rs}]$ and $[p_{rs}]$, respectively. In Fig. 4, $N_{r0}(\xi,\eta) = N_{r1}(\xi,\eta) = \cdots = N_{rl}(\xi,\eta)$. If the number of elements in every row are different from each other, we have $N_{r0}(\xi,\eta) \neq N_{r1}(\xi,\eta) \neq \cdots \neq N_{rl}(\xi,\eta)$. $N_{rs}(\xi,\eta)$ does not satisfy the Kronecker delta property, but it is constricted to interpolate the node values $\tilde{p}_{ij}$, i.e.,

$$\tilde{p}_j = P(\xi_j,\eta_j) = \sum_i N_i(\xi_j,\eta_j)\hat{p}_i \tag{16}$$

where $\tilde{p}_j$ is an arbitrary vector element corresponding to the node values $\tilde{p}_{ij}$.

Substituting Eq. (16) into Eq. (15) with inverse transformation, we have

$$\begin{aligned} P(\xi,\eta) &= \sum_i N_i(\xi,\eta) \sum_j \left([N]_{ij}^{-1}\tilde{p}_j \right) = \sum_i \sum_j N_i(\xi,\eta)[N]_{ij}^{-1}\tilde{p}_j \\ &= \sum_j \tilde{N}_j(\xi,\eta)\tilde{p}_j \end{aligned} \tag{17}$$

where $\tilde{N}_j(\xi,\eta) = \sum_i N_i(\xi,\eta)[N]_{ij}^{-1}$, $[N]_{ij} = [N_i(\xi_j,\eta_j)]$.

To use Eq. (17), it is easy to construct the B-spline approximation functions of boundary variables: $u(s)$ and $q(s)$, respectively, such as

$$u(\xi,\eta) = \sum_i \tilde{N}_i(\xi,\eta)\tilde{u}(\xi_i,\eta_i) \tag{18}$$

$$q(\xi,\eta) = \sum_i \tilde{N}_i(\xi,\eta)\tilde{q}(\xi_i,\eta_i) \tag{19}$$

where $u(\xi,\eta)$ and $q(\xi,\eta)$ are the 2-D parametric expressions of $u(s)$ and $q(s)$, respectively.

Substituting Eqs. (18) and (19) in the Eq. (13), we have

$$\sum_{uv} I_{uv}^{(1)} + \sum_{uv} I_{uv}^{(2)} = 0 \tag{20}$$

where $I_{uv}^{(1)}$ and $I_{uv}^{(2)}$ are expressed as

$$I_{uv}^{(1)} = \sum_l \left(\int_0^1 \int_0^1 (\tilde{N}_j(\xi,\eta) - \tilde{N}_j(\xi_0,\eta_0))q^s(\xi,\eta)J(\xi,\eta)d\xi\, d\eta \right)(\tilde{u}_j)_l \tag{21}$$

$$I_{uv}^{(2)} = \sum_l \left(\int_0^1 \int_0^1 \tilde{N}_j(\xi,\eta)u^s(\xi,\eta)J(\xi,\eta)d\xi\, d\eta \right)(\tilde{t}_j)_l \tag{22}$$

where $(\tilde{u}_j)_l = \tilde{u}_j(\xi_l,\eta_l)$ and $(\tilde{t}_j)_l = \tilde{t}_j(\xi_l,\eta_l)$.

Then, Eq. (13) can be written as a matrix form

$$\mathbf{H}\tilde{\mathbf{u}} - \mathbf{G}\tilde{\mathbf{q}} = \mathbf{0} \tag{23}$$

3.3. Exact geometric information

The bodies for the analysis in the 3-D potential BIEs are only a kind of boundary representation (B-rep) geometric models. The boundary surfaces of the bodies are built with bivariate B-spline or NURBS functions in our isogeometric analysis schema. To calculate the integrals of the Eq. (20), geometric information is required, such as the spatial coordinates of the boundary surfaces and Jacobian. This information can be analytically calculated from

Eqs. (5) or (6) in fact, so it is exact. For example, Fig. 5 shows a body enclosed by one bivariate quadratic NURBS surface. The control net is shown in Fig. 5(b), which is corresponding to the parametric mesh in the Fig. 5(a). The exact spatial coordinates of $p_{ij}(x,y,z)$ in Fig. 5(b) can be directly estimated by Eq. (6) with the given parametric coordinates of (ξ_i,η_j) in Fig. 5(a). Other exact geometric information of the body, such as Jacobian and out normal can also be found from the partial derivatives of Eq. (6).

4. Numerical examples

Two 3-D B-spline geometric models are applied in the solution of potential BIEs to illustrate the accuracy and convergence of B-spline isogeometric analysis. Note that these models in the BIEs are based on B-rep, i.e., these bodies are only composed by boundary surfaces. That is a distinct advantage over isogeometric analysis implemented in FEM where 3-D geometric models must be constructed by trivariate B-spline functions. To evaluate the error of numerical results, a 'global' L_2 norm error, normalized by $|v|_{\max}$, is defined by [17]

$$e=\frac{1}{|v|_{\max}}\sqrt{\frac{1}{N}\sum_{i=1}^{N}(v_i^{(e)}-v_i^{(n)})^2} \tag{24}$$

where $|v|_{\max}$ is the maximum value of sample points, the superscripts (e) and (n) refer to the exact and numerical solutions, respectively. To assess the accuracy of numerical results in the current isogeometric analysis, we use the following three analytical fields, which are taken from Ref. [17]:

(i) Quadratic solution

$$u=-2x^2+y^2+z^2 \tag{25}$$

(ii) Cubic solution

$$u=x^3+y^3+z^3-3yx^2-3xz^2-3zy^2 \tag{26}$$

In all cases, BIEs generated from Laplace's equation $\nabla^2 u=0$ are solved, combined with reasonable prescribed boundary conditions corresponding to the above analytical solutions.

4.1. Potential problem for a sphere shell

A semisphere shell is firstly used for discussion, which is constructed by three quadratic NURBS surfaces: two semisphere surfaces and one disk surface. The body and its main size are shown in Fig. 6. Fig. 6(b) and (c) are, respectively, the planform and side elevation of the body. The red dashes in the two figures are used to denote the location of reference numerical solutions in the following illustration. In this case, the Dirichlet boundary conditions corresponding to the exact solutions (Eqs. (25) and (26)) are imposed on the surface of the semisphere shell.

The global and local bivariate B-spline are applied for approximation of boundary variables. The surface mesh in Fig. 7(a) is subdivided according to the parametric definition of global bivariate B-spline. Because of the restriction of global tensor product, the mesh must be kept with a uniform number of nodes in every meridian direction along the woof direction. As a result,

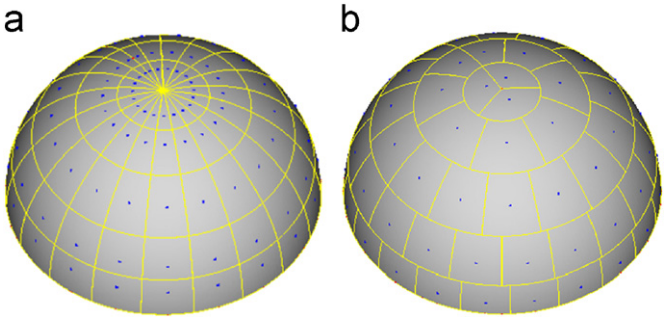

Fig. 7. Two different mesh models for the semisphere shell: (a) mesh according to global B-spline definition and (b) mesh according to local B-spline definition.

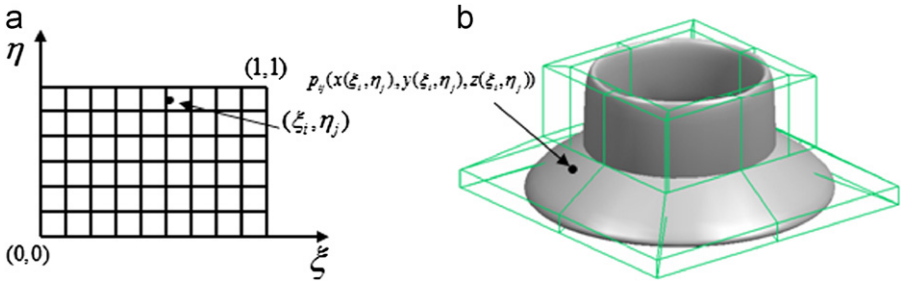

Fig. 5. A body constructed by one bivariate quadratic NURBS surface.

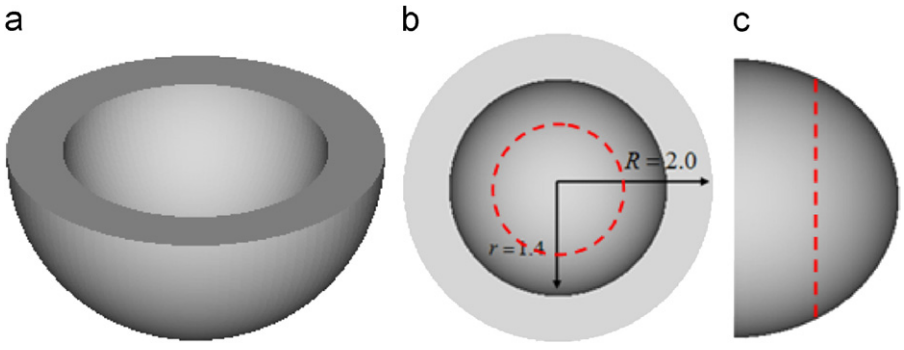

Fig. 6. A semisphere shell and its main size: (a) semisphere shell, (b) planform of semisphere shell and (c) side elevation of semisphere shell. (For interpretation of the references to color in this figure, the reader is referred to the web version of this article.)

many of nodes huddle in the poles of the two semisphere surfaces that further results in many nearly singular and singular integrals needing to be solved in the potential BIE. Whereas, the mesh in Fig. 7(b) allows variable number of nodes allocated in every meridian, so there are lesser nodes in the poles.

Table 1 describes the numerical errors and computational time estimated from the two fashion of mesh in Fig. 7. The L_2 errors of nodal values of q is denoted by Err_q evaluated by Eq. (24) and time required for constructing the coefficient matrices is denoted by Mat_t for various analytical fields. From the table, we can clearly see that the nodal values evaluated from 510 nodes on the body surface in the local B-spline definition is more exact than that from 580 nodes in the global definition. And much time for computation is also saved in the local definition compared with the global. It indicates that the transformation of global bivariate B-spline to local is meaningful for improvement of the computational efficiency and exactness in the potential BIE.

In Figs. 8 and 9, the quadratic local B-spline as the approximation function is used to determine the convergence rates of our method. The normal flux q on the red dashes in Fig. 6(b) and (c) are considered. Three groups of nodes: 96 nodes; 184 nodes; 256 nodes, are used to discretize the semisphere shell surface. In Fig. 8, cubic boundary condition corresponding to Eq. (26) is imposed on the body surfaces. And the numerical results obtained from 184 nodes and 256 nodes are in good agreement with the exact solutions, even if the first data from 96 nodes has little fluctuation. In Fig. 9, quadratic boundary condition corresponding to Eq. (25) is imposed on the body. And the numerical results finally are convergent to the exact solutions by few of nodes. The two figures testify that the local B-spline is a stable approximation method to approximate boundary variables in potential BIE.

Table 1
The L_2 errors of q together with computational time from two meshes.

Number of nodes	Analytical field	Degree of B-spline	Err_q (%)	Mat_t (s)
510(Local B-spline)	u=quadratic	Two degree	**0.04775**	**489**
		Three degree	**0.02022**	**516**
	u=cubic	Two degree	**0.1085**	**532**
		Three degree	**0.09563**	**534**
580 (Global B-spline)	u=quadratic	Two degree	0.0588	2497
		Three degree	0.02622	2627
	u=cubic	Two degree	0.1638	2462
		Three degree	0.1007	2715

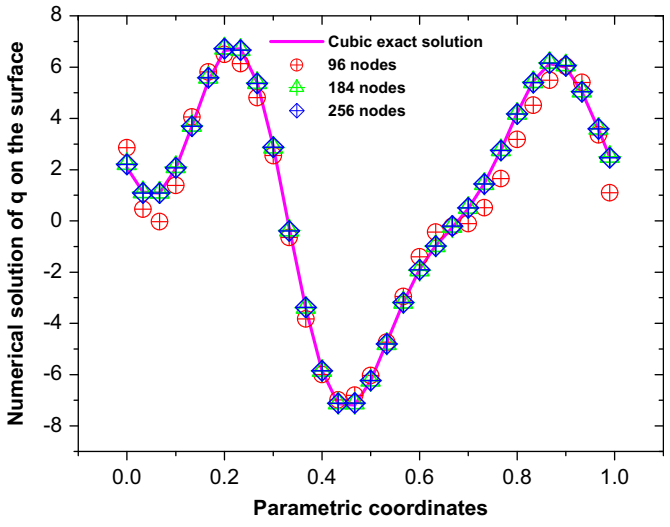

Fig. 8. Variation of normal flux q along the red dashes on the r=1.4 semisphere surface. (For interpretation of the references to color in this figure legend, the reader is referred to the web version of this article.)

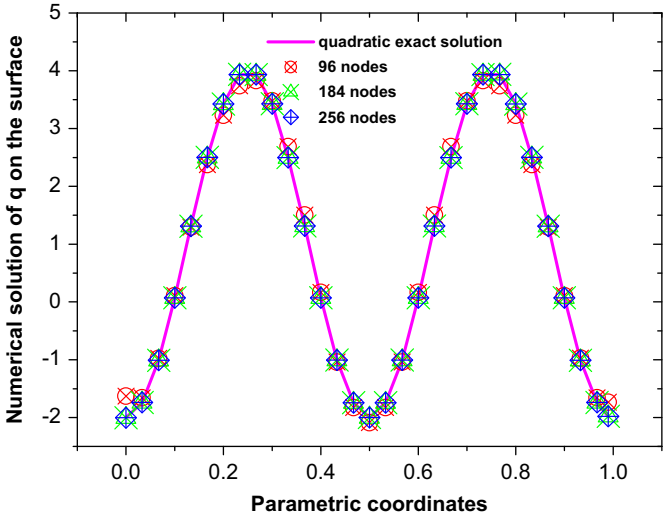

Fig. 9. Variation of normal flux q along the red dashes on the R=2.0 semisphere surface. (For interpretation of the references to color in this figure legend, the reader is referred to the web version of this article.)

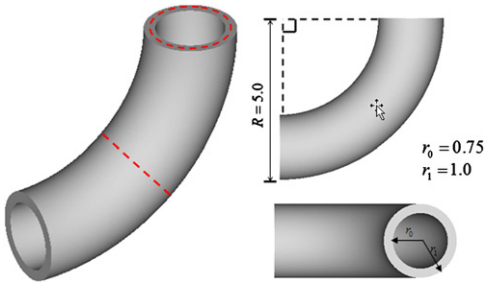

Fig. 10. A tube and its main size. (For interpretation of the references to color in this figure, the reader is referred to the web version of this article.)

4.2. Potential problem for a tube

In this case, a tube is used for analysis, which is composed by four NURBS surfaces: two toroidal and two disk surfaces. The body and its main size are shown in Fig. 10. The Dirichlet boundary conditions corresponding to the exact solution (Eq. (25)) is imposed on the surface of the tube. There are three sets of nodes: (a) 276 nodes; (b) 526 nodes; (c) 892 nodes; to be used for discretization of the body surfaces, these mesh models are presented in Fig. 11. The global quadratic bivariate B-splines is applied for approximation of boundary variables.

In order to determine the convergence rate, the normal flux q on the toroidal and disk surfaces labeled by red dashes in Fig. 10 is considered. Note that the labeled end surface is a slightness surfaces comparing with the tube where many nearly singulars will be required for evaluation. Fig. 12 shows that the numerical results obtained from quadratic B-spline approximation are convergent to the exact solutions following the increment of nodes on the body surfaces, even if the results obtained from the discretization of 276 nodes and 526 nodes fluctuate. The numerical results evaluated by the same B-spline on the large toroidal surface are in good agreement with the cubic exact solutions in Fig. 13, even the calculation from 276 nodes. The comparison between Figs. 12 and 13 indicates that to evaluate exactly the

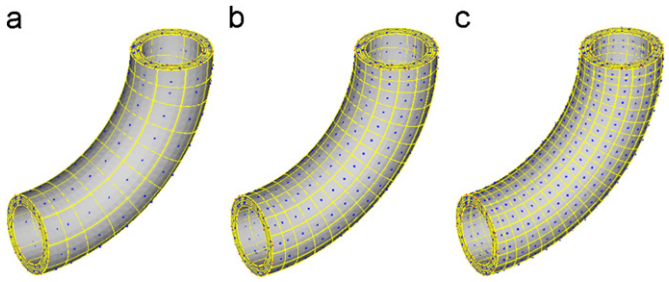

Fig. 11. Three mesh models of the tube: (a) 276 nodes, (b) 526 nodes and (c) 892 nodes.

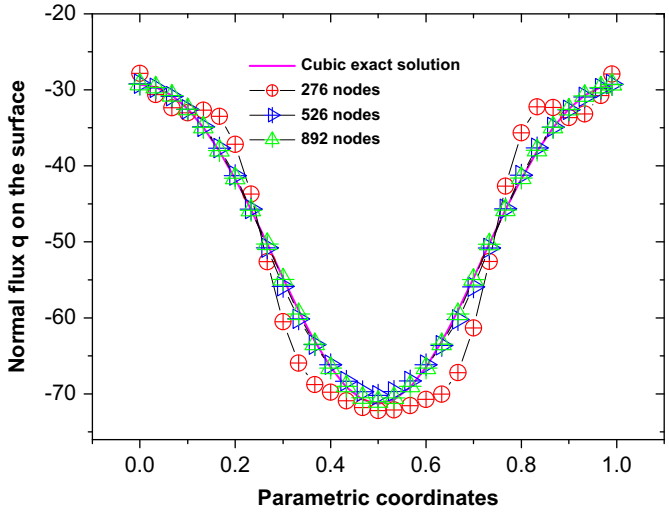

Fig. 12. Variation of normal flux q along the red dashes on the end surface. (For interpretation of the references to color in this figure legend, the reader is referred to the web version of this article.)

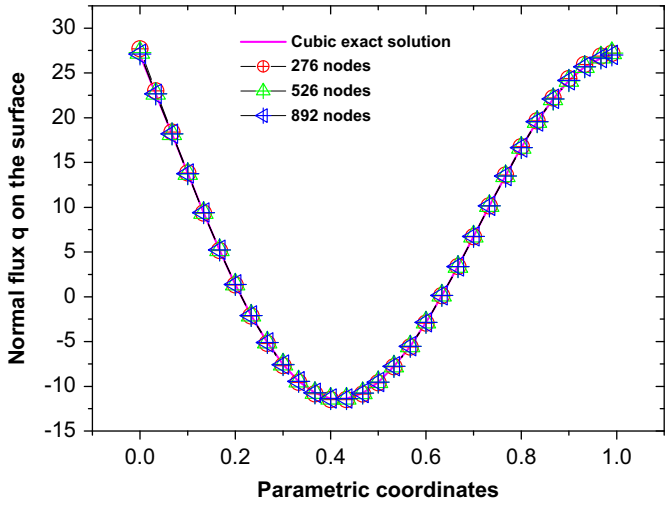

Fig. 13. Variation of normal flux q along the red dashes on the toroidal surface. (For interpretation of the references to color in this figure legend, the reader is referred to the web version of this article.)

results on a small size surface is more difficult than that on large size surface. In fact, computation of small size feature problem is still a challenge issue in engineering problem. But B-spline here performs well. This numerical example testifies again that B-spline has stronger potential in approximation.

5. Conclusions

The conception of isogeometric analysis has been successfully implemented in the 3-D potential BIE. It is a meaningful attempt to seamlessly integrate CAD modeling and BEA and to simplify the communication of mesh refinement with CAD model. The first goal of isogeometric analysis has been achieved in the potential BIE, which is to be geometrically exact no matter how coarse the discretization. The new implementation in BIE can be considered as improvement and generalization of traditional BEA.

Basis function form B-spline or NURBS has been applied for CAD modeling and analysis of 3-D potential BIE. For particular shape, the mesh model of body produces many of singular points restricted by the global tensor product fashion of B-spline. The local bivariate B-spline has been proposed to avoid the computation of many nearly singular and singular integrals on singular points. In approximation of boundary variables, the B-spline bivariate functions are fitting type functions, i.e. they lack the Kronecker delta property, so an inverse transformation is performed to convert them into ones of interpolation type.

Numerical tests have demonstrated that the isogeometric analysis for solution of the 3-D potential BIE is feasible. High convergence rates and high exactness obtained from the tests indicate that the isogeometric analysis has the stronger potential to be expanded into other areas of BEA.

The proposed local B-spline has the potential to simplify the mesh refinement, which is another mentioned goal in isogeometric analysis. To use local B-spline for mesh refinement and for other engineering problems is an ongoing work.

To deal with the large-scale computations for complicated geometric bodies, the Fast Multipole Method (FMM) [18–20] can be applied to reduce the computation expense. And this is also planned.

Acknowledgments

This work was supported in part by the National Science Foundation of China under Grant number 10972074 and in part by the National 973 Project of China under Grant number 2010CB328005.

References

[1] Hughes TJR, Cottrell JA, Bazilevs Y. Isogeometric analysis: CAD, finite elements, NURBS, exact geometry and mesh refinement. Comput Methods Appl Mech Eng 2005;194:4135–95.
[2] Cottrell JA, Hughes TJR, Reali A. Studies of refinement and continuity in isogeometric analysis. Comput Methods Appl Mech Eng 2007;196:4160–83.
[3] Cottrell JA, Reali A, Bazilevs Y, Hughes TJR. Isogeometric analysis of structural vibrations. Comput Methods Appl Mech Eng 2006;195:5257–96.
[4] Bazilevs Y, Calo VM, Zhang Y, Hughes TJR. Isogeometric fluid–structure interaction analysis with applications to arterial blood flow. Comput Methods Appl Mech Eng 2006;38:310–22.
[5] Bazilevs Y, Beirao de Veiga L, Cottrell JA, Hughes TJR, Sangalli G. Isogeometric analysis: approximation, stability and error estimates for h-refined meshes. Math Models Methods Appl Sci 2006;16:1031–90.
[6] Zhang Y, Bazilevs Y, Goswami S, Bajaj C, Hughes TJR. Patient-specific vascular NURBS modeling for isogeometric analysis of blood flow. Comput Methods Appl Mech Eng 2007;196:2943–59.
[7] Sederberg TW, Zheng J, Bakenov A, Nasri A. T-splines and T-NURCCSs. ACM Trans Graph 2003;22:477–84.
[8] Brebbia CA, Wrobel LC. Boundary element method for fluid flow. Adv Water Res 1979;2:83–9.
[9] Cabral JJSP, Wrobel LC, Brebbia. CA. A BEM formulation using B-splines: II-multiple knots and non-uniform blending functions. Eng Anal Boundary Elem 1991;8:51–5.
[10] Kitagawa Koichi, Brebbia Carlos A, Luiz CWrobel, Tanaka Masataka. Boundary element analysis of viscous flow by penalty function formulation. Eng Anal Boundary Elem 1986;3:194–200.
[11] DeFigueiredo TGB, Brebbia. CA. A new variational boundary element model for potential problems. Eng Anal Boundary Elem 1991;8:45–50.

[12] Gavankar P, Henderson MR. Graph-based extraction of protrusions and depressions from boundary representation. Comput-Aided Des 1990;22(7): 442–50.
[13] Falcidieno B, Giannini F. Automatic recognition and representation of shape-based features in a geometric modeling system. Comput Vision Graphics Image Process 1989;48:93–123.
[14] Zhang JM, Qin XY, Han X, Li GY. A boundary face method for potential problems in three dimensions. Int J Numer Methods Eng 2009;80:320–37.
[15] Bazilevs Y, Calo VM, Cottrell JA, Evans JA, Hughes TJR, Lipton S, et al. Isogeometric analysis using T-splines. Comput Methods Appl Mech Eng 2010;199:229–63.
[16] Sederberg TW, Zheng J, Bakenov A, Nasri A. T-splines and T-NURCCSs. ACM Trans Graph 2003;22(3):477–84.
[17] Chati MK, Mukherjee S. The boundary node method for three-dimensional problems in potential theory. Int J Numer Methods Eng 2000;47:1523–47.
[18] Zhang JM, Tanaka M, Endo M. The hybrid boundary node method accelerated by fast multipole method for 3D potential problems. Int J Numer Methods Eng 2005;63:660–80.
[19] Zhang JM, Tanaka M. Fast HdBNM for large-scale thermal analysis of CNT-reinforced composites. Comput Mech 2008;41:777–87.
[20] Zhang JM, Tanaka M. Adaptive spatial decomposition in fast multipole method. J Comput Phys 2007;226:17–28.